# Structure−Activity Relationship of Sulfonyl Piperazine LpxH Inhibitors Analyzed by an LpxE-Coupled Malachite Green Assay

Minhee Lee,[†] Jinshi Zhao,[‡] Seung-Hwa Kwak,[†] Jae Cho,[‡] Myungju Lee,[§] Robert A. Gillespie,[‡] Do-Yeon Kwon,[†] Hyunji Lee,[†][iD] Hyun-Ju Park,[∥][iD] Qinglin Wu,[‡] Pei Zhou,*[,‡][iD] and Jiyong Hong*[,†][iD]

[†]Department of Chemistry, Duke University, 124 Science Drive, Box 90346, Durham, North Carolina 27708, United States
[‡]Department of Biochemistry, Duke University Medical Center, Box 3711, Durham, North Carolina 27710, United States
[§]College of Pharmacy, Ewha Womans University, 52, Ewhayeodae-gil, Seodaemun-gu, Seoul 03760, Republic of Korea
[∥]School of Pharmacy, Sungkyunkwan University, 2066 Seobu-ro, Jangan-gu, Suwon, Gyeonggi-do 16419, Republic of Korea

S **Supporting Information**

ABSTRACT: The UDP-2,3-diacylglucosamine pyrophosphatase LpxH in the Raetz pathway of lipid A biosynthesis is an essential enzyme in the vast majority of Gram-negative pathogens and an excellent novel antibiotic target. The ^{32}P-radioautographic thin-layer chromatography assay has been widely used for analysis of LpxH activity, but it is inconvenient for evaluation of a large number of LpxH inhibitors over an extended time period. Here, we report a coupled, nonradioactive LpxH assay that utilizes the recently discovered *Aquifex aeolicus* lipid A 1-phosphatase LpxE for quantitative removal of the 1-phosphate from lipid X, the product of the LpxH catalysis; the released inorganic phosphate is subsequently quantified by the colorimetric malachite green assay, allowing the monitoring of the LpxH catalysis. Using such a coupled enzymatic assay, we report the biochemical characterization of a series of sulfonyl piperazine LpxH inhibitors. Our analysis establishes a preliminary structure−activity relationship for this class of compounds and reveals a pharmacophore of two aromatic rings, two hydrophobic groups, and one hydrogen-bond acceptor. We expect that our findings will facilitate the development of more effective LpxH inhibitors as potential antibacterial agents.

KEYWORDS: LpxH, LpxE, lipid A, Gram-negative bacteria, novel antibiotics, enzyme-coupled assay
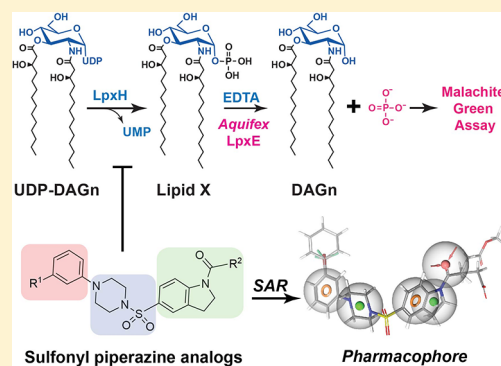
The emergence of multi-drug-resistant nosocomial Gram-negative pathogens poses a serious threat to public health and highlights the urgent need for novel antibiotics to overcome established resistance mechanisms.[1,2] The outer membrane of Gram-negative bacteria consists of an asymmetric bilayer, with the inner leaflet enriched of phospholipids and the outer leaflet decorated with lipopolysaccharide (LPS) or lipooligosaccharide (LOS). The membrane anchor of LPS and LOS is a unique saccharolipid, known as lipid A (endotoxin), that shields bacteria from the damage of external detergents and antibiotics and causes Gram-negative septic shock during bacterial infection.[3] Constitutive biosynthesis of lipid A by the Raetz pathway is required for the viability and fitness of virtually all Gram-negative bacteria in nature and in the human host.[3−6] As the Raetz pathway has never been exploited by commercial antibiotics, lipid A biosynthetic enzymes are excellent novel antibiotic targets.

Lipid A biosynthesis in *Escherichia coli* is accomplished by nine enzymes, of which the first six enzymes are essential.[3,5] Although the chemical transformation of lipid A biosynthesis is conserved throughout all Gram-negative organisms, the fourth step of the pathway, the cleavage of the pyrophosphate group of UDP-2,3-diacylglucosamine (UDP-DAGn) to form lipid X, is carried out by three functional orthologs that do not coexist: LpxH in β- and γ-proteobacteria,[7] LpxI in α-proteobacteria,[8] and LpxG in Chlamydiae (Figure 1).[9] Among these three enzymes, LpxH is most widespread, functioning in the majority (∼70%) of Gram-negative bacteria and in all of the WHO-listed priority Gram-negative pathogens,[1] rendering LpxH an excellent antibiotic target.

Recently, a small molecule inhibitor containing the sulfonyl piperazine scaffold (referred to as AZ1 below; chemical structure shown in Figure 1) was discovered to display antibiotic activity against efflux-deficient *E. coli* strains.[10] Based on the analysis of spontaneous resistance mutations, the target was identified as LpxH. Consistent with this designation, overexpression of LpxH resulted in a significant elevation of the minimum inhibitory concentration.[10]

To exploit LpxH in antibiotic development, a robust activity assay is required to establish the structure−activity relationship (SAR) of lead compounds. The previously reported ^{32}P-autoradiographic thin-layer chromatography (TLC) assay[9,11] is the most sensitive method for evaluation of LpxH activity and
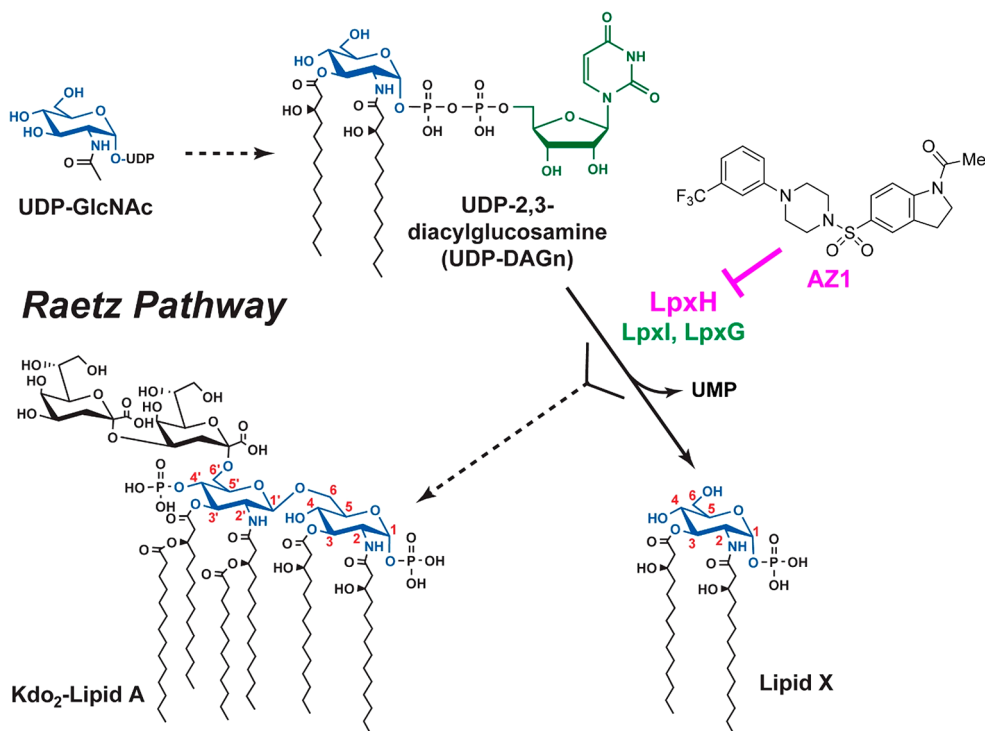
Figure 1. Lipid A biosynthetic (Raetz) pathway. The conversion of UDP-2,3-diacylglucosamine (UDP-DAGn) to lipid X is catalyzed by LpxH (colored in pink) in the vast majority of human Gram-negative pathogens or its functional paralogs LpxI and LpxG (both colored in green).
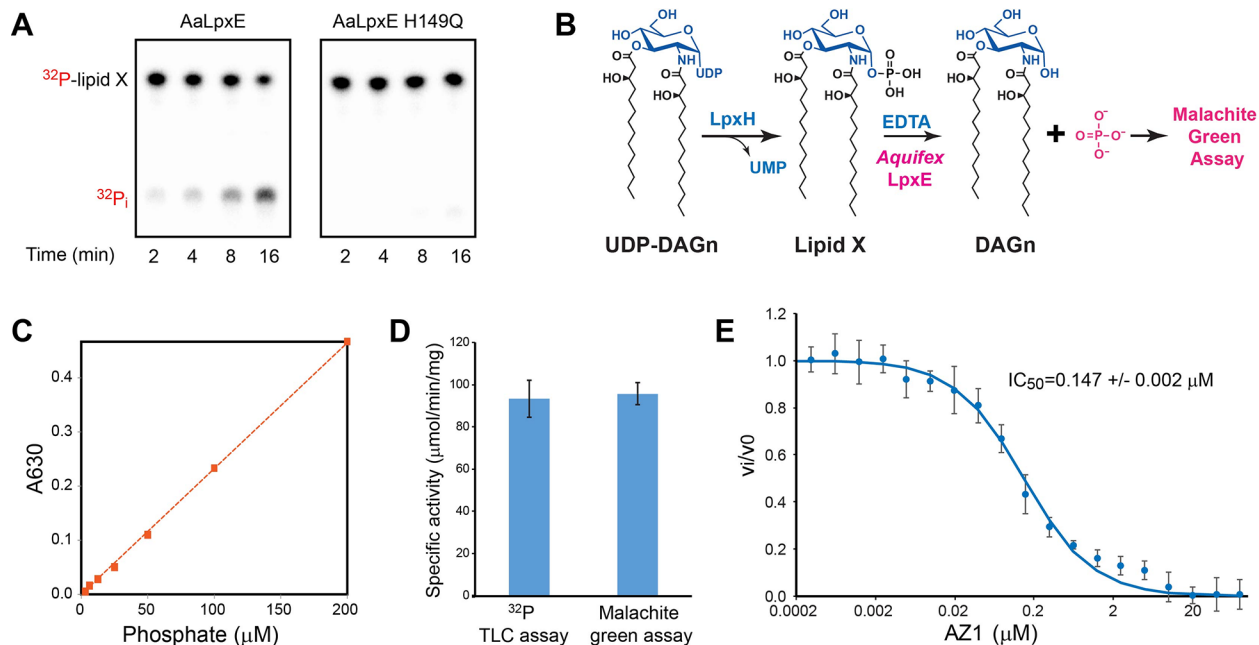

Figure 2. AaLpxE-coupled, malachite green assay for LpxH. (A) AaLpxE, but not the catalytically deficient H149Q mutant, efficiently dephosphorylates lipid X to yield free inorganic phosphate. (B) AaLpxE-coupled malachite green assay for analyzing LpxH activity. (C) Standard curve of inorganic phosphate in the LpxH reaction conditions containing detergents and Mn^{2+}. (D) Comparison of the specific LpxH activity determined by ^{32}P-autoradiographic TLC and AaLpxE-coupled malachite green assays. (E) Dose-dependent inhibition of *E. coli* LpxH by AZ1 determined by the enzyme-coupled malachite green assay, yielding an IC_{50} value of $0.147 \pm 0.002\ \mu M$. Error bars represent standard deviations from triplicate measurements.

inhibition. However, due to the short half-life of ^{32}P and the complicated procedure for preparation and purification of the ^{32}P-labeled substrate,[9,11] such a radioactive assay is inconvenient for evaluating a large number of LpxH inhibitors over an extended period. In order to facilitate the development of

LpxH-targeting antibiotics, here we report the development of a nonradioactive assay for convenient measurements of LpxH activity. Furthermore, we present the modular synthesis of a series of sulfonyl piperazine LpxH inhibitors and the

establishment of a preliminary SAR and pharmacophore model for this class of compounds.

■ RESULTS AND DISCUSSION

Development of a Nonradioactive, Colorimetric Coupled Assay for LpxH Activity. Despite the high sensitivity of the conventional ^{32}P-autoradiographic TLC assay that has been used to identify catalytically important residues and establish the metal dependence of LpxH and its functional paralog LpxG,[9,11] its application to the inhibition analysis of a large number of compounds over an extended period is hindered by the limited half-life of the ^{32}P-radiolabeled substrate and the complexity of the substrate preparation. To address these challenges, we developed a nonradioactive, colorimetric assay for evaluating the LpxH activity and inhibition. This assay utilizes the recent discovery of the lipid A 1-phosphatase LpxE from *Aquifex aeolicus* (AaLpxE).[12] We found that in addition to its reported activity on Kdo$_2$-lipid A, AaLpxE, but not the catalytically inactive H149Q mutant, efficiently and quantitatively dephosphorylates lipid X, the product of the LpxH catalysis (Figure 2A). As LpxH is a Mn^{2+}-dependent hydrolase, whereas AaLpxE is not, the conversion of UDP-DAGn to lipid X and UMP catalyzed by LpxH can be quenched by the treatment of EDTA. Subsequent addition of AaLpxE to the reaction mixture converts lipid X to DAGn and inorganic phosphate (Figure 2B). The release of the inorganic phosphate is then probed by the colorimetric malachite green assay through the formation of a complex between malachite green, molybdate, and free phosphate to yield color change.

Because our assay includes detergents (e.g., Triton X-100) and Mn^{2+}, we first investigated whether the malachite green assay is compatible with such an assay condition. A phosphate standard curve was generated for concentrations between 0 and 200 μM in the standard enzymatic assay buffer (20 mM Tris-HCl pH 8.0, 0.5 mg/mL BSA, 0.02% Triton X-100, 1 mM MnCl$_2$) (Figure 2C). We found that the colorimetric signal is linear with respect to the added phosphate concentration, suggesting that the presence of detergents and Mn^{2+} does not adversely affect the malachite green assay. Using a substrate concentration of 100 μM, the specific activity of LpxH measured by the AaLpxE-coupled malachite green assay (95.7 ± 5.2 μmol/min/mg) is indistinguishable from that obtained from the ^{32}P-autoradiographic TLC assay (93.5 ± 8.7 μmol/min/mg) (Figure 2D), suggesting that the coupled assay is suitable for quantitative measurements of LpxH activity. Using this coupled malachite green assay, we were able to determine a dose-dependent inhibition curve of *E. coli* LpxH by AZ1, yielding an IC$_{50}$ value of 0.147 ± 0.002 μM (Figure 2E).

Synthesis of AZ1 Analogues toward *E. coli* LpxH. Encouraged by the robustness of the newly developed LpxH activity assay, we embarked on the synthesis of a series of AZ1 analogues in order to establish a preliminary SAR of AZ1. The structure of AZ1 is highly modular (Figure 1): it contains a trifluoromethyl-substituted phenyl ring and an *N*-acetyl indoline group that are connected by a central sulfonyl piperazine linker. We envisioned that a variety of AZ1 analogues could be prepared by coupling readily available *N*-phenyl-substituted piperazines to *N*-acyl indoline sulfonyl chlorides, as illustrated in Figure 3. We anticipated that a detailed SAR analysis of AZ1 analogues would help identify essential chemical motifs and minimal structural requirements for LpxH inhibition, which will in turn allow chemical
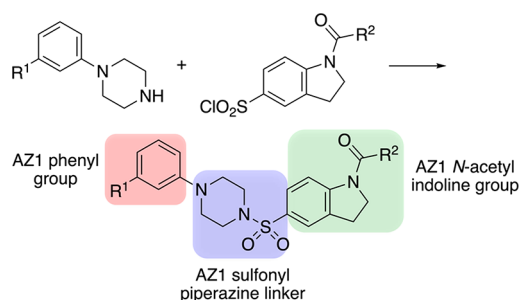

Figure 3. Convergent synthesis of AZ1 analogues.

modifications to enhance potency and specificity, decrease off-target effects, and improve drug performance.
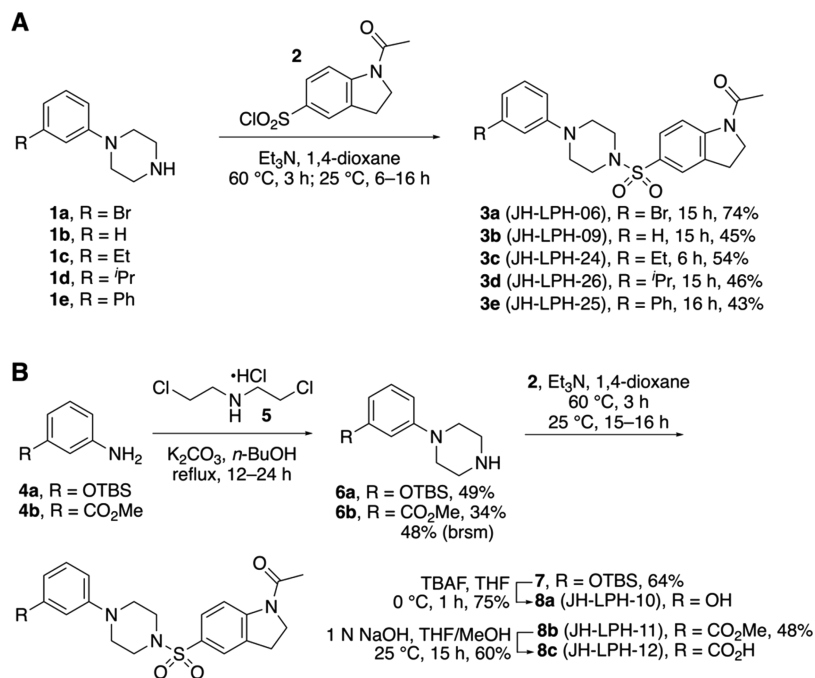
AZ1 Phenyl Group Analogues. To gain insights into the importance of the trifluoromethyl group of AZ1 in LpxH inhibition, we prepared AZ1 phenyl group analogues by replacing the trifluoromethyl group with various functional groups, including halogen, alkyl, and carboxylate groups. Commercially available *m*-substituted phenyl piperazines (**1a−e**) were coupled to the commercially available 1-acetyl-5-indolinesulfonyl chloride **2** (Scheme 1A). The coupling reaction proceeded smoothly in the presence of Et$_3$N to afford **3a−e** (JH-LPH-06, -09, -24, -26, and -25) in 43−74% yield.

Next, treatment of 3-(*tert*-butyldimethylsilyloxy)aniline **4a**[13] with 2,2′-dichlorodiethylamine hydrochloride (**5**) gave the desired 1-(3-((*tert*-butyldimethylsilyl)oxy)phenyl)piperazine (**6a**) (Scheme 1B).[14] Coupling of **6a** and **2** followed by final TBS deprotection gave the phenol analogue **8a** (JH-LPH-10) in 75% yield. Carboxylate analogues **8b** (JH-LPH-11) and **8c** (JH-LPH-12) were prepared from 3-carbomethoxyaniline (**4b**) in a similar manner (Scheme 1B).

AZ1 N-Acetyl Indoline Group Analogues. To investigate the role of the *N*-acetyl and indoline groups of AZ1 in LpxH inhibition, we generated a series of AZ1 *N*-acetyl indoline group analogues. First, we prepared the *N*-acetylsulfanil analogue **11** (JH-LPH-15) by replacing the indoline ring of AZ1 with aniline, but keeping the *N*-acetyl group (Scheme 2A). We also replaced the *N*-acetyl group with extended carbonyl chains such as 1,3-diketohydroxamic acid **13** (JH-LPH-16) in order to assess the effect of chain elongation and potential metal binding by the hydoxamic acid group in **13** on activity. The synthesis of **13** began with coupling of **9** to commercially available 4-acetamidobenzenesulfonyl chloride (**10**). Then, Ac deprotection of the *N*-acetylsulfanil analogue **11** (JH-LPH-15) followed by coupling of the resulting aniline with monoethyl malonate gave the oxoacetate **12**. Compound **12** was subsequently hydrolyzed by LiOH to afford the corresponding carboxylic acid. PyBOP-mediated coupling with NH$_2$OTBS successfully provided the desired hydroxamic acid analogue **13** (JH-LPH-16) but in low yield (35%) (Scheme 2A). Attempts to install the hydroxamic acid group using ethyl chloroformate and NH$_2$OH·HCl were not successful. In a similar manner, the synthesis of the phenyloxalamide analogue (**17**, JH-LPH-17) began with coupling of **14** with methyl chlorooxoacetate to give the oxoacetate **15** (Scheme 2B). Basic hydrolysis of **15** by LiOH followed by installation of a hydroxamic acid group completed the synthesis of **17** (JH-LPH-17).

To mimic the hydrogen bonding capability of the *N*-acetyl group, we coupled **9** with 3-carboxybenzne sulfonyl chloride (**18a**) and 3-(carbomethoxy)benzenesulfonyl chloride (**18b**)

Scheme 1. Synthesis of AZ1 Phenyl Group Analogues

A

1a, R = Br
1b, R = H
1c, R = Et
1d, R = ^{i}Pr
1e, R = Ph

3a (JH-LPH-06), R = Br, 15 h, 74%
3b (JH-LPH-09), R = H, 15 h, 45%
3c (JH-LPH-24), R = Et, 6 h, 54%
3d (JH-LPH-26), R = ^{i}Pr, 15 h, 46%
3e (JH-LPH-25), R = Ph, 16 h, 43%

B

4a, R = OTBS
4b, R = CO$_2$Me

6a, R = OTBS, 49%
6b, R = CO$_2$Me, 34%
48% (brsm)

TBAF, THF ⌐ 7, R = OTBS, 64%
0 °C, 1 h, 75% └ 8a (JH-LPH-10), R = OH

1 N NaOH, THF/MeOH ⌐ 8b (JH-LPH-11), R = CO$_2$Me, 48%
25 °C, 15 h, 60% └ 8c (JH-LPH-12), R = CO$_2$H

to provide **19a** (JH-LPH-20) and **19b** (JH-LPH-21), respectively (Scheme 2C).

We also prepared the indoline 5-oxobutanoic acid analogues **22a** (JH-LPH-07) and **22b** (JH-LPH-08) by modifying both the trifluoromethyl and *N*-acetyl groups of AZ1, as illustrated in Scheme 2D. Coupling of the known sulfonyl chloride **21**[15] with 1-(3-bromophenyl)piperazine (**1a**) provided the desired **22a** (JH-LPH-07), which was subsequently hydrolyzed to afford **22b** (JH-LPH-08).

AZ1 Sulfonyl Piperazine Linker Analogues. In order to probe whether sulfonyl piperazine linker of AZ1 provides the optimal distance between the trifluoromethylphenyl ring and the *N*-acetyl indoline group and whether it interacts with LpxH, we prepared several sulfonamide linker analogues.

First, we prepared two larger core ring analogues **26a** (JH-LPH-18) and **26b** (JH-LPH-19) by replacing the piperazine group of AZ1 with 1,4-diazacycloheptane and 1,5-diazacyclooctane, respectively (Scheme 3).[16] We expected **26a** (JH-LPH-18) and **26b** (JH-LPH-19) would provide insights into the effect of ring size and conformation of AZ1 analogues on LpxH inhibition.

Next, in order to evaluate the effect of structural rigidity, we synthesized the flexible acyclic linker analogue **28** (JH-LPH-14). The known N^1-(3-(trifluoromethyl)phenyl)ethane-1,2-diamine (**27**)[17] was treated with 1-acetyl-5-indolinesulfonyl chloride (**2**) to afford the desired acyclic analogue **28** (JH-LPH-14) in 80% yield (Scheme 4A). The one-carbon homologated analogue **30** (JH-LPH-23) was prepared in a similar manner. To take advantage of the potential binding of the kojic acid group to the di-Mn^{2+} cluster of the LpxH active site, we designed and synthesized the AZ1 kojic acid analogue **36** (JH-LPH-04) starting from the known phosphonate **31**[18] and aldehyde **32**[19] (Scheme 4B). To define the role of the sulfonamide group of AZ1, we used the standard EDC−HOBt amide coupling condition and prepared the corresponding amide analogue **38** (JH-LPH-22) (Scheme 4C).

Analysis of SAR of AZ1 Analogues. Among the tested AZ1 analogues, the *m*-bromophenyl piperazine analogue (JH-LPH-06) showed the strongest inhibition of LpxH activity (Table 1). It inhibited 74% of LpxH activity at 1 μM. Several other AZ1 analogues (JH-LPH-07, JH-LPH-08, and JH-LPH-25) also showed a useful level of LpxH inhibitory activity. The LpxH activity assay data provided several valuable insights into the SAR.

First, among AZ1 phenyl group analogues, analogues with a hydrophobic substituent on the trifluoromethyl phenyl ring (e.g., JH-LPH-06 and JH-LPH-25) were active, but analogues with a polar functional group, such as the phenol analogue JH-LPH-10 and the benzoic acid analogue JH-LPH-12, were inactive. A bulky hydrophobic *m*-substituent group was beneficial for the activity (JH-LPH-06 vs JH-LPH-09). These data indicated the importance of the hydrophobicity and size of the *m*-substituent on the phenyl ring in LpxH inhibitory activity.

Extended *N*-acyl groups were well tolerated and only slightly reduced the activity of AZ1 analogues (JH-LPH-06 vs JH-LPH-07). Interestingly, the sulfanilide analogue (JH-LPH-15) was active, indicating that the indoline ring might not be essential to LpxH inhibition. However, the extend sulfanilide analogues (JH-LPH-16 and JH-LPH-17) were less active than JH-LPH-15, and the benzoic acid analogues (JH-LPH-20 and JH-LPH-21) were inactive.

The comparison of AZ1, JH-LPH-18, and JH-LPH-19 revealed that the six-membered piperazine ring is optimal for the LpxH inhibition by AZ1. Larger ring analogues (JH-LPH-18 and JH-LPH-19) were less potent than AZ1. The more flexible or extended piperazine analogues (JH-LPH-4, JH-LPH-14, and JH-LPH-23) were essentially inactive, suggesting that both the rigidity of the piperazine linker and the orientation of the trifluoromethyl-substituted phenyl ring are crucial to the AZ1 activity. Surprisingly, the amide analogue JH-LPH-22 was inactive, indicating that the sulfonamide linker is important for the AZ1 activity either by maintaining the

**Scheme 2. Synthesis of AZ1 *N*-Acetyl Indoline Group Analogues**
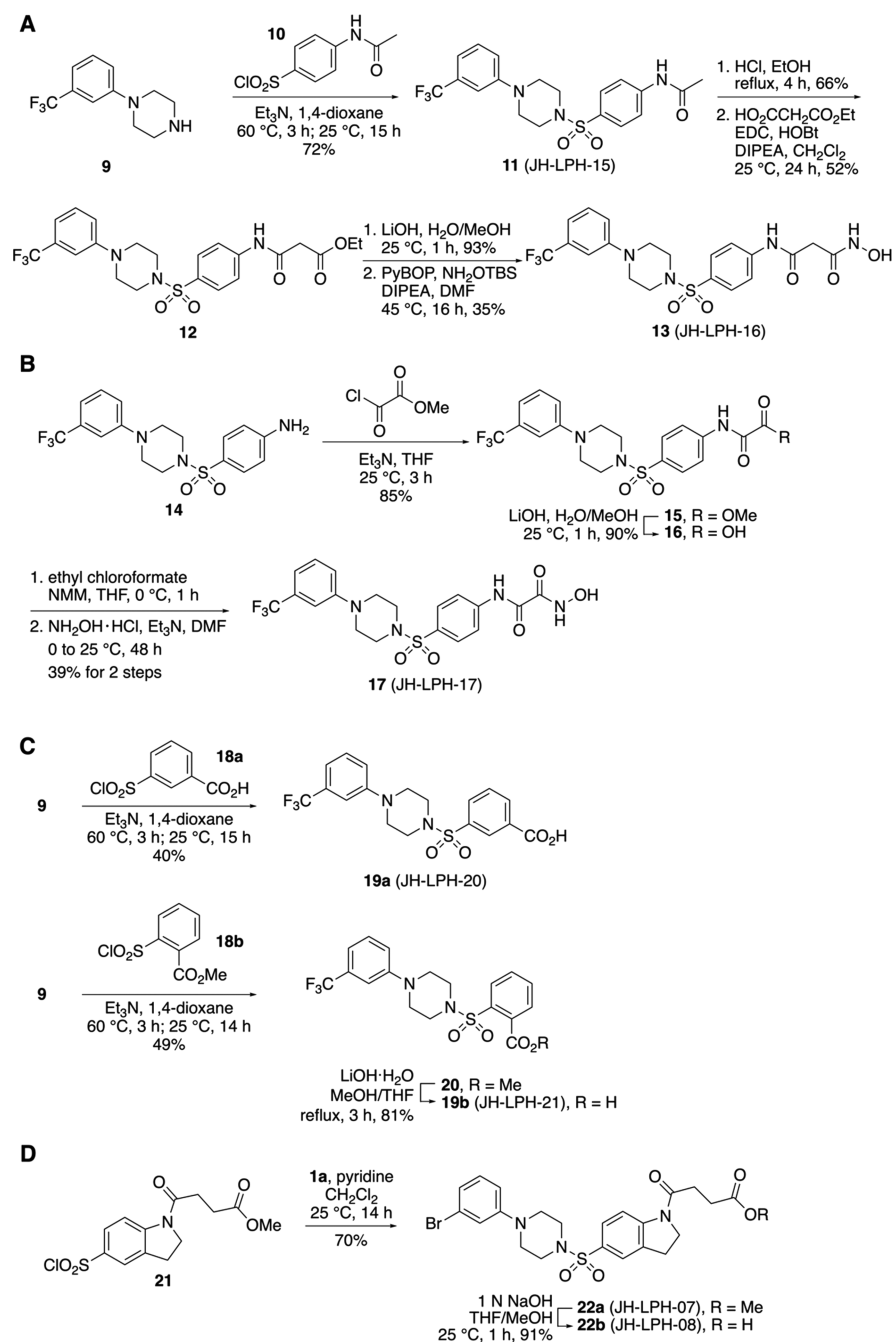
optimal compound geometry or by direct interacting with LpxH, or both.

Pharmacophore Model of LpxH Inhibitors. Pharmacophore models have been used successfully for data mining and the design of small molecule libraries. Statistically significant pharmacophore studies based on the analysis of active and inactive analogues have been used to identify essential and unfavorable steric regions and electronic requirements.[20]
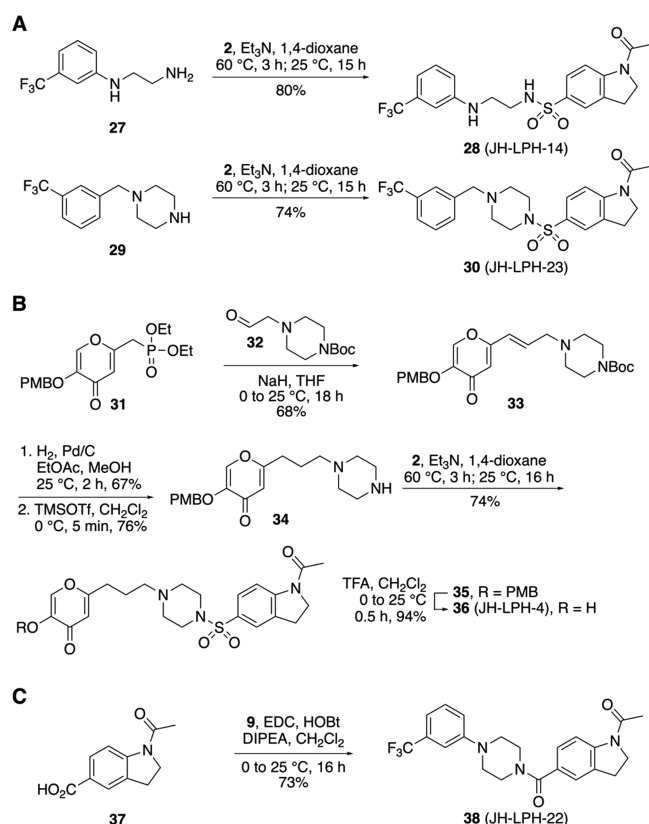
We generated a pharmacophore model of LpxH inhibitors by analyzing the SAR and mapping common structural features of the five most active compounds (>45% inhibition at 1 μM; AZ1, JH-LPH-06, JH-LPH-07, JH-LPH-08, and JH-LPH-25). A total of 50 five-point hypotheses were generated for LpxH inhibitors, respectively, by requiring all active ligands matched to the generated hypotheses. The initial hypotheses were

evaluated by scoring both active and inactive ligands. Although inactive ligands were not involved in model generation, they were used to eliminate hypotheses that do not distinguish between active and inactive compounds, which is especially useful when all active ligands share a common structural scaffold. Figure 4A shows the pharmacophore with the highest adjusted scores mapped onto the most active compound AZ1. The pharmacophore model is represented with *AHHRR*, indicating that it has one hydrogen-bond acceptor (A), two hydrophobic groups (H), and two aromatic rings (R). Two hydrophobic groups and one hydrogen-bond acceptor are mapped to the piperazine ring, the indoline ring, and the carbonyl group, respectively. These molecular features are shared by all active ligands, whereas inactive analogues, including JH-LPH-19 that has a single atom difference from

Scheme 3. Synthesis of Analogues with Larger Core Ring Linkers
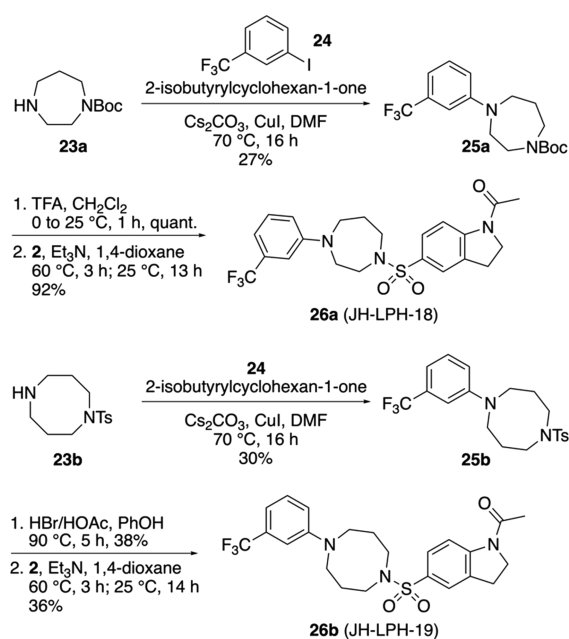
Scheme 4. Synthesis of AZ1 Analogues with Flexible Linkers and an Amide Linker

AZ1, have poor overlaps with the pharmacophore model of LpxH inhibitors (Figure 4B).

While this study was in progress, Bohl and co-workers reported a docking model of AZ1 for LpxH.[21] In their model, the trifluoromethyl-substituted phenyl ring is located close to the active site consisting primarily of hydrophilic residues

involved in the recognition of the 1-phosphoglucosamine headgroup and the β-hydroxyl groups of the 2,3-diacyl chains of the product lipid X; additionally, the trifluoromethyl group points toward the solvent-accessible open space above the active site, suggesting that substitution of the trifluoromethyl group with polar functional groups should be well tolerated. However, our SAR analysis and pharmacophore model show that replacement of the hydrophobic trifluoromethyl group with a polar functional group (e.g., the hydroxyl group in JH-LPH-10 or the carboxylate group in JH-LPH-12) is detrimental to the inhibitory activity of AZ1, whereas a bulky hydrophobic substitution (e.g., the bromo group in JH-LPH-06 or the phenyl group in JH-LPH-25) is well tolerated. Furthermore, terminal polar functional groups (such as carboxylates) of the N-acyl chain on the indoline ring (e.g., JH-LPH-07 and JH-LPH-08) are well accepted, and the carbonyl oxygen of the N-acetyl group on the indoline ring is a highlighted hydrogen-bond acceptor in our pharmacophore model, which would likely interact with polar residues in the active site rather than hydrophobic residues in the acyl chain chamber of LpxH. Taken together, our SAR analysis and pharmacophore model reveal several inconsistencies of the AZ1 docking model proposed by Bohl and co-workers[21] and instead support a model that AZ1 is oriented with the trifluoromethyl group away from the active site and with the N-acetyl indoline close to the active site.

■ CONCLUSION

The first six enzymes in the Raetz pathway of lipid A biosynthesis are essential enzymes and viable antibiotic targets. So far, most inhibitor development has focused on LpxC, the second enzyme of the pathway, due to the early discovery of lead compounds in the 1990s.[22] Inhibition of late-stage lipid A enzymes such as LpxH may be uniquely advantageous as accumulation of lipid A precursors such as UDP-DAGn is toxic, which provides a second mechanism of cell killing in addition to disruption of lipid A biosynthesis.[23,24] In order to facilitate the discovery of effective LpxH inhibitors, we have developed a nonradioactive, colorimetric malachite green assay that utilizes the unexpected ability of the recently discovered AaLpxE enzyme to quantitatively desphosphorylate lipid X to yield DAGn and free inorganic phosphate. Using this assay, we have biochemically characterized a series of LpxH inhibitors based on the sulfonyl piperazine scaffold of AZ1, established a preliminary SAR, and identified the pharmacophore of this series of LpxH inhibitors. These efforts will ultimately contribute to the design and development of more potent LpxH inhibitors, as has been demonstrated for LpxC inhibitors.[25,26]

■ EXPERIMENTAL SECTION

For the synthesis of AZ1 analogues, see the Supporting Information for details.

Cloning and Purification of *E. coli* LpxH. The *E. coli* LpxH gene was cloned into a modified pET30 vector (EMD Millipore) containing an N-terminal His₁₀-SUMO-fusion protein. The sequence verified plasmid was used to transform BL21(DE3)STAR competent *E. coli* cells (ThermoFisher). Cells were grown in the Luria broth medium at 37 °C until OD₆₀₀ reached 0.5, induced with 1 mM isopropyl-β-D-thiogalactopyranoside (IPTG) for 3 h, and then harvested by centrifugation.

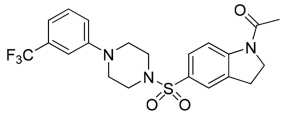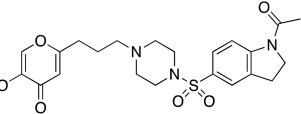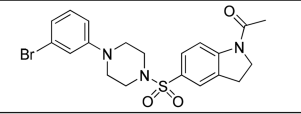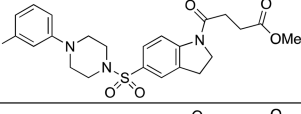**Table 1. Specific Activity of *E. coli* LpxH in the Presence of AZ1 Analogues**
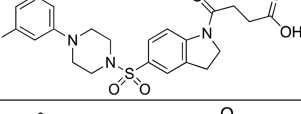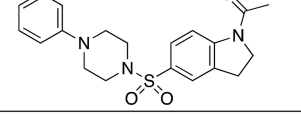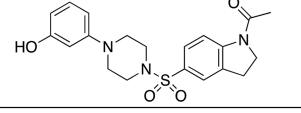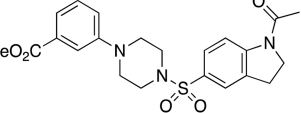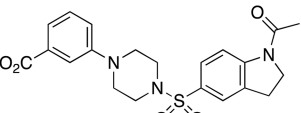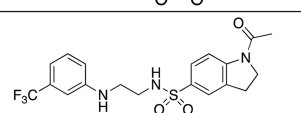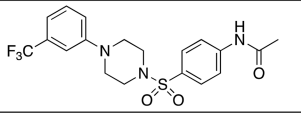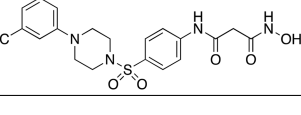
Compounds	Structure	10 μM compound		1 μM compound	
		Activity (μmol/min/mg)[a]	Percentage Activity	Activity (μmol/min/mg)[a]	Percentage Activity
DMSO		96.0 ± 4.7	N/A	96.0 ± 4.7	N/A
AZ1		5.7 ± 2.5	6 ± 3	16.0 ± 0.7	17 ± 1
JH-LPH-04		109.5 ± 5.0	114 ± 8	ND	ND
JH-LPH-06		22.6 ± 5.8	24 ± 6	25.3 ± 8.0	26± 8
JH-LPH-07		40.0 ± 7.9	42 ± 8	50.6 ± 10.5	53 ± 11
JH-LPH-08		23.5 ± 7.0	24 ± 7	50.0 ± 10.7	52 ± 11
JH-LPH-09		31.1 ± 8.2	32 ± 9	105.7 ± 9.1	110 ± 11
JH-LPH-10		87.1 ± 14.1	91 ± 15	ND	ND
JH-LPH-11		34.3 ± 6.7	36 ± 7	98.5 ± 6.3	103 ± 8
JH-LPH-12		125.5 ± 6.7	131 ± 9	ND	ND
JH-LPH-14		142.6 ± 13.8	149 ± 16	ND	ND
JH-LPH-15		28.6 ± 10.8	30 ± 11	67.3 ± 7.1	70 ± 8
JH-LPH-16		52.8 ± 25.5	55 ± 27	ND	ND

Table 1. continued

Compounds	Structure	10 μM compound		1 μM compound	
JH-LPH-17		38.9 ± 8.8	41 ± 9	116.6 ± 1.4	121 ± 6
JH-LPH-18		89.9 ± 19.7	94 ± 21	ND	ND
JH-LPH-19		143.3 ± 12.3	149 ± 15	ND	ND
JH-LPH-20		93.9 ± 5.3	98 ± 7	ND	ND
JH-LPH-21		103.9 ± 11.7	108 ± 13	ND	ND
JH-LPH-22		98.0 ± 10.9	102 ± 12	ND	ND
JH-LPH-23		83.3 ± 2.5	87 ± 5	ND	ND
JH-LPH-24		20.5 ± 1.6	21 ± 2	64.9 ± 7.8	68 ±9
JH-LPH-25		23.0 ± 2.9	24 ± 3	42.9 ± 9.8	45 ± 10
JH-LPH-26		28.2 ± 2.5	29 ± 3	66.8 ± 2.1	70 ± 4

[a]Data are mean values of three independent experiments. Errors represent standard deviation. N/A: not applicable. ND: not determined.

All of the purification procedures were carried out at 4 °C. Cells from 8 L of induced culture were resuspended and lysed in 120 mL of the lysis buffer containing 20 mM HEPES (pH 8.0) and 200 mM NaCl using French Press. Cell debris were removed by centrifugation at 10000g for 40 min. To the supernatant, n-dodecyl-β-D-maltopyranoside (DDM) was added to reach a final concentration of 1.5% (w/v; 29 mM). After 2 h of incubation, membranes were removed by centrifugation at 100000g for 1 h. Supernatant from the centrifugation was diluted to a final volume of 240 mL with the lysis buffer and added to a column containing 20 mL of HisPur Ni-NTA resin (ThermoFisher) pre-equilibrated with 100 mL of the purification buffer containing 20 mM HEPES (pH 8.0), 200 mM NaCl, and 0.0174% (w/v; 0.34 mM) DDM. The

column was washed with 250 mL of the purification buffer containing 50 mM imidazole, and the His$_{10}$-SUMO-LpxH was eluted with 150 mL of the purification buffer containing 300 mM imidazole. The eluted protein sample was concentrated and further purified with size-exclusion chromatography (Superdex 200; GE Healthcare Life Sciences) in the purification buffer.

[32]P-Autoradiographic TLC Assay for AaLpxE. The ^{32}P-radiolabeled and unlabeled lipid X and the wild-type and H149Q AaLpxE were prepared as previously described.[12,27] To investigate the AaLpxE activity toward lipid X as the substrate, a 10 μL reaction mixture containing 50 mM Tris-HCl (pH 7.5), 0.05% Triton X-100, 100 μM lipid X, and 500 cpm/μL ^{32}P-lipid X was preincubated at 30 °C, and the reaction was
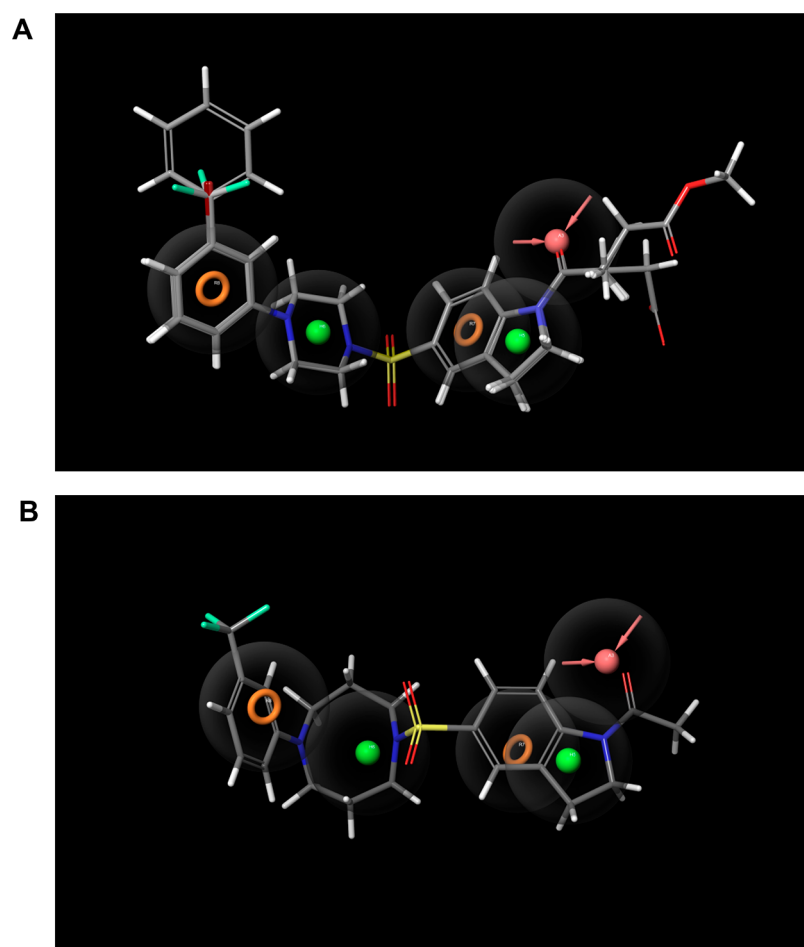
Figure 4. Pharmacophore model for LpxH inhibitors (green, hydrophobic groups; orange, aromatic rings; rose, hydrogen-bond acceptor). (A) Alignment of five most active LpxH inhibitors (AZ1, JH-LPH-06, JH-LPH-07, JH-LPH-08, and JH-LPH-25) to the pharmacophore. (B) Alignment of an inactive ligand (JH-LPH-19) to the pharmacophore.

initiated by addition of 1 μg/mL purified AaLpxE. The reactions were quenched by spotting 2 μL reaction mixture on the TLC plate at the specified time points. The plate was dried and developed in a solvent system consisting of chloroform, methanol, acetic acid, and water (25:15:4:4, v/v), followed by analysis using the Typhoon FLA 7000 PhosphorImager scanner equipped with ImageQuant software (GE Healthcare).

Enzymatic Assay for LpxH. To examine the compatibility of the malachite green assay kit (Sigma catalog number MAK307) with our assay condition, the phosphate standard provided with the kit was diluted into our assay reaction buffer containing 20 mM Tris-HCl pH 8.0, 0.5 mg/mL BSA, 0.02% Triton X-100, and 1 mM $MnCl_2$. The linear colorimetric response to a range of phosphate concentrations up to 200 μM was confirmed.

The autoradiographic assay protocol for LpxH was adapted from the previous report[9] with minor modifications, including the use of our current assay buffer conditions as described above and the reaction incubation temperature at 37 °C instead of 30 °C.

A typical assay for LpxH using the coupled malachite green assay protocol contained the assay reaction buffer (20 mM Tris-HCl pH 8.0, 0.5 mg/mL BSA, 0.02% Triton X-100, and 1 mM $MnCl_2$) with 100 μM UDP-DAGn and 5% DMSO or inhibitors. The reaction mixtures were preincubated at 37 °C for 10 min before LpxH was added with a 5-fold dilution to

start the reaction at 37 °C. At the desired reaction time points, an aliquot of 20 μL of reaction mixture was removed and added to a well in 96-well half-area plate containing 5 mM EDTA (final concentration) to quench the LpxH reaction. Then purified AaLpxE was added to a final concentration of 5 μg/mL. The plate was incubated at 37 °C for 30 min followed by addition of formic acid to a final concentration of 3.75 M to quench the reaction. The malachite green reagent was added with a 5-fold dilution, and the absorbance at 620 nm was measured after 30 min incubation at room temperature. The amount of free inorganic phosphate from hydrolyzed lipid X was determined from the phosphate standard curve and used to calculate the specific activity of the SUMO-LpxH fusion protein.

For determination of IC$_{50}$, up to 80 μM of AZ1 compound was added to the assay reaction containing 5% DMSO. Our preliminary analysis showed that despite the strong inhibition of LpxH activity by AZ1 at 1 μM, there existed significant levels of enzymatic activity at elevated compound concentrations beyond 10 μM. Therefore, the protocol for IC$_{50}$ determination was adjusted to include 10% DMSO instead of 5% DMSO for the dose−response analysis of AZ1 to mitigate the concern of limited compound solubility. The increase of DMSO concentration had minimal impact on the specific activity of LpxH. The IC$_{50}$ value was extracted from fitting of the dose−response curve of $v_i/v_0 = 1/(1 + [I]/\text{IC}_{50})$.

Pharmacophore Modeling. The pharmacophore model of LpxH inhibitors was generated based on total number of 22 analogues that were tested for their inhibition effects against LpxH (Table 1). The molecular structures were sketched and built with Maestro.11.2 (Schrödinger, NY). The pharmacophore model was generated with the "Develop Pharmacophore Model" module of Phase. Low-energy conformations of LpxH inhibitors were generated by LigPrep of Schrödinger. The pharmacophore model was developed with the most active training set compounds, which are defined as "active ligands" for pharmacophore generation. Features of hydrogen-bond acceptor and donor, hydrophobic, negative, positive, and aromatic rings were located in the pharmacophore model. Pharmacophores with tree features that match all active ligands were generated by using a tree-based partitioning technique (Phase, version 11.2; Schrödinger) with maximum tree depth of five. The generated pharmacophore hypotheses were scored with default parameters.

ASSOCIATED CONTENT

S Supporting Information

The Supporting Information is available free of charge on the ACS Publications website at DOI: 10.1021/acsinfecdis.8b00364.

General experimental procedures with spectroscopic and analytical data (PDF)

AUTHOR INFORMATION

Corresponding Authors
*E-mail: peizhou@biochem.duke.edu.
*E-mail: jiyong.hong@duke.edu.

ORCID
Hyunji Lee: 0000-0001-8463-5078
Hyun-Ju Park: 0000-0001-6802-1412
Pei Zhou: 0000-0002-7823-3416
Jiyong Hong: 0000-0002-5253-0949

Author Contributions
M.L. and J.Z. contributed equally; P.Z. and J.H. conceived the project, designed the overall experimental strategy, and analyzed and discussed the results; M.L., M.J.L., D.K., and H.L. synthesized the small molecules used in this study; S.-H.K. and H.-J.P. performed pharmacophore modeling and other computational studies for the project; R.A.G. made the initial observation of the lipid X activity for AaLpxE. Q.W. purified AaLpxE; J.C. purified LpxH; J.Z., Q.W., and J.C. purified lipid X and UDP-DAGn. J.Z. developed the AaLpxE-coupled enzymatic assay and characterized the inhibitory effect of LpxH inhibitors; P.Z. and J.H. wrote the manuscript with input from all the authors and held overall responsibility for the study.

Notes
The authors declare no competing financial interest.

ACKNOWLEDGMENTS

REFERENCES

(1) WHO Global priority list of antibiotic-resistant bacteria to guide research, discovery, and development of new antibiotics; World Health Organization, 2017.

(2) Boucher, H. W., Talbot, G. H., Bradley, J. S., Edwards, J. E., Gilbert, D., Rice, L. B., Scheld, M., Spellberg, B., and Bartlett, J. (2009) Bad bugs, no drugs: no ESKAPE! An update from the Infectious Diseases Society of America. *Clin. Infect. Dis.* 48 (1), 1−12.

(3) Raetz, C. R. H., and Whitfield, C. (2002) Lipopolysaccharide endotoxins. *Annu. Rev. Biochem.* 71, 635−700.

(4) Barb, A. W., and Zhou, P. (2008) Mechanism and inhibition of LpxC: an essential zinc-dependent deacetylase of bacterial lipid A synthesis. *Curr. Pharm. Biotechnol.* 9 (1), 9−15.

(5) Zhou, P., and Zhao, J. (2017) Structure, inhibition, and regulation of essential lipid A enzymes. *Biochim. Biophys. Acta, Mol. Cell Biol. Lipids* 1862 (11), 1424−1438.

(6) Whitfield, C., and Trent, M. S. (2014) Biosynthesis and export of bacterial lipopolysaccharides. *Annu. Rev. Biochem.* 83, 99−128.

(7) Babinski, K. J., Ribeiro, A. A., and Raetz, C. R. (2002) The *Escherichia coli* gene encoding the UDP-2,3-diacylglucosamine pyrophosphatase of lipid A biosynthesis. *J. Biol. Chem.* 277 (29), 25937−25946.

(8) Metzger, L. E., and Raetz, C. R. (2010) An alternative route for UDP-diacylglucosamine hydrolysis in bacterial lipid A biosynthesis. *Biochemistry* 49 (31), 6715−6726.

(9) Young, H. E., Zhao, J., Barker, J. R., Guan, Z., Valdivia, R. H., and Zhou, P. (2016) Discovery of the elusive UDP-Diacylglucosamine hydrolase in the lipid A biosynthetic pathway in *Chlamydia trachomatis. mBio* 7 (2), e00090-16.

(10) Nayar, A. S., Dougherty, T. J., Ferguson, K. E., Granger, B. A., McWilliams, L., Stacey, C., Leach, L. J., Narita, S., Tokuda, H., Miller, A. A., Brown, D. G., and McLeod, S. M. (2015) Novel antibacterial targets and compounds revealed by a high-throughput cell wall reporter assay. *J. Bacteriol.* 197 (10), 1726−1734.

(11) Young, H. E., Donohue, M. P., Smirnova, T. I., Smirnov, A. I., and Zhou, P. (2013) The UDP-diacylglucosamine pyrophosphohydrolase LpxH in lipid A biosynthesis utilizes Mn^{2+} cluster for catalysis. *J. Biol. Chem.* 288 (38), 26987−27001.

(12) Zhao, J., An, J., Hwang, D., Wu, Q., Wang, S., Gillespie, R. A., Yang, E. G., Zhou, P., and Chung, H. S. The Lipid A 1-phosphatase, LpxE, Functionally Connects Multiple Layers of Bacterial Envelope Biogenesis. Submitted for publication.

(13) Schiaffino-Ortega, S., Lopez-Cara, L. C., Rios-Marco, P., Carrasco-Jimenez, M. P., Gallo, M. A., Espinosa, A., Marco, C., and Entrena, A. (2013) New non-symmetrical choline kinase inhibitors. *Bioorg. Med. Chem.* 21 (22), 7146−7154.

(14) Zhao, D., Xie, H., Bai, C., Liu, C., Hao, C., Zhao, S., Yuan, H., Luo, C., Wang, J., Lin, B., Zheng, J., and Cheng, M. (2016) Design, synthesis and biological evaluation of N,N-3-phenyl-3-benzylamino-propanamide derivatives as novel cholesteryl ester transfer protein inhibitor. *Bioorg. Med. Chem.* 24 (8), 1589−1597.

(15) Wu, J., Lawrence, N. J., and Sebti, S. M. Indoline scaffold Shp-2 inhibitors, their preparation, and use for cancer treatment. PCT Int. Appl. WO 2010011666A2, 2010.

(16) Shafir, A., and Buchwald, S. L. (2006) Highly selective room-temperature copper-catalyzed C-N coupling reactions. *J. Am. Chem. Soc.* 128 (27), 8742−8743.

(17) Lv, K., Li, L., Wang, B., Liu, M., Wang, B., Shen, W., Guo, H., and Lu, Y. (2017) Design, synthesis and antimycobacterial activity of novel imidazo[1,2-a]pyridine-3-carboxamide derivatives. *Eur. J. Med. Chem.* 137, 117−125.

(18) Chen, Y. H., Lu, P. J., Hulme, C., and Shaw, A. Y. (2013) Synthesis of kojic acid-derived copper-chelating apoptosis inducing agents. *Med. Chem. Res.* 22 (2), 995−1003.

(19) Johnson, M., Antonio, T., Reith, M. E., and Dutta, A. K. (2012) Structure-activity relationship study of N(6)-(2-(4-(1H-Indol-5-yl)-piperazin-1-yl)ethyl)-N(6)-propyl-4,5,6,7-tetrahydroben zo[d]-thiazole-2,6-diamine analogues: development of highly selective D3 dopamine receptor agonists along with a highly potent D2/D3 agonist

and their pharmacological characterization. *J. Med. Chem.* 55 (12), 5826−5840.

(20) Yang, S. Y. (2010) Pharmacophore modeling and applications in drug discovery: challenges and recent advances. *Drug Discovery Today* 15 (11−12), 444−450.

(21) Bohl, T. E., Ieong, P., Lee, J. K., Lee, T., Kankanala, J., Shi, K., Demir, O., Kurahashi, K., Amaro, R. E., Wang, Z., and Aihara, H. (2018) The substrate-binding cap of the UDP-diacylglucosamine pyrophosphatase LpxH is highly flexible, enabling facile substrate binding and product release. *J. Biol. Chem.* 293 (21), 7969−7981.

(22) Onishi, H. R., Pelak, B. A., Gerckens, L. S., Silver, L. L., Kahan, F. M., Chen, M. H., Patchett, A. A., Galloway, S. M., Hyland, S. A., Anderson, M. S., and Raetz, C. R. H. (1996) Antibacterial agents that inhibit lipid A biosynthesis. *Science* 274 (5289), 980−982.

(23) Babinski, K. J., Kanjilal, S. J., and Raetz, C. R. (2002) Accumulation of the lipid A precursor UDP-2,3-diacylglucosamine in an *Escherichia coli* mutant lacking the *lpxH* gene. *J. Biol. Chem.* 277 (29), 25947−25956.

(24) Richie, D. L., Takeoka, K. T., Bojkovic, J., Metzger, L. E., Rath, C. M., Sawyer, W. S., Wei, J. R., and Dean, C. R. (2016) Toxic Accumulation of LPS Pathway Intermediates Underlies the Requirement of LpxH for Growth of *Acinetobacter baumannii* ATCC 19606. *PLoS One* 11 (8), No. e0160918.

(25) Kalinin, D. V., and Holl, R. (2017) LpxC inhibitors: a patent review (2010−2016). *Expert Opin. Ther. Pat.* 27 (11), 1227−1250.

(26) Lee, C. J., Liang, X., Wu, Q., Najeeb, J., Zhao, J., Gopalaswamy, R., Titecat, M., Sebbane, F., Lemaitre, N., Toone, E. J., and Zhou, P. (2016) Drug design from the cryptic inhibitor envelope. *Nat. Commun.* 7, 10638.

(27) Radika, K., and Raetz, C. R. (1988) Purification and properties of lipid A disaccharide synthase of *Escherichia coli*. *J. Biol. Chem.* 263 (29), 14859−14867.